

# Mechanical and Microstructural Characterization of a Titanium-based Ti-6Al-2Cr-2Ni Alloy Produced by SPS Sintering for Use in the Aerospace Industry

Sarra Zioual<sup>1\*</sup>, Youcef Khelfaoui<sup>1</sup>, Djamel Amari<sup>2</sup>, Salim Abdelli<sup>1</sup>, Atmane Djermoune<sup>3</sup>

<sup>1</sup> Université de Bejaia, Faculté de Technologie, Laboratoire de Mécanique, Matériaux et Energétique (L2ME), 06000 Bejaia, Algeria

<sup>2</sup> Université de Bejaia, Faculté de Technologie, Laboratoire de Génie de L'environnement (LGE), 06000 Bejaia, Algeria

<sup>3</sup> Scientific and Technical Research Center in Physical and Chemical Analyses (CRAPC), BP 384 Bou-Ismaïl, RP 42004 Tipaza, Algeria

\* Corresponding author, e-mail: [sarra.zioual@univ-bejaia.dz](mailto:sarra.zioual@univ-bejaia.dz)

Received: 19 May 2025, Accepted: 08 December 2025, Published online: 17 December 2025

## Abstract

Titanium-based alloys are widely applied in the aerospace industry thanks to their excellent strength-to-weight ratio, good corrosion resistance and thermal stability. In this study, a Ti-6Al-2Cr-2Ni alloy was elaborated by Spark Plasma Sintering (SPS), a technique derived from powder metallurgy that enables rapid, controlled densification. Sintering was carried out at 1000 °C under 30 MPa for 8 minutes in an inert atmosphere. A thermal annealing treatment at 550 °C was then applied to optimize microstructure and mechanical properties. Microstructural characterization by scanning electron microscopy (SEM), combined with EDS elemental analysis, revealed a significant reduction in porosity and progressive homogenization of the alloying elements after treatment. X-ray diffraction (XRD) confirmed the presence of a majority of  $\alpha$ -Ti phase, associated with intermetallic compounds. Mechanically, Vickers microhardness measurements showed an increase in hardness after annealing, while instrumented indentation enabled Young's modulus to be reliably determined. These results indicate that the Ti-6Al-2Cr-2Ni alloy developed by SPS is a promising alternative to standard alloys such as Ti-6Al-4V, offering improved microstructural controllability, interesting mechanical properties and thermal optimization potential for advanced aerospace applications.

## Keywords

FE-SEM, microhardness, SPS, titanium alloy, XRD, Young's modulus

## 1 Introduction

Today's aerospace industry is faced with increasingly stringent technological requirements, dictated by the need to reduce fuel consumption, increase aircraft range, and improve reliability in extreme environments. In this context, the development of materials that are light, strong and capable of withstanding severe operating conditions is a major scientific and industrial challenge [1, 2]. Aircraft engines, in particular combustion chambers, turbine blades and disks, are subject to particularly severe temperature, mechanical load and corrosion conditions. As a result, the choice of materials is becoming a determining factor in performance [3]. Recent research confirms this approach, with increased focus on titanium-based alloys capable of ensuring safe operation at high temperatures and under severe mechanical stress [4].

Titanium alloys, and more specifically  $\alpha$  and  $\alpha + \beta$  alloys, are widely used in aerospace structures and engine

components for their excellent compromise between reduced density, mechanical strength and corrosion resistance [5]. TA6V (Ti-6Al-4V) remains the reference alloy in industry, but its high-temperature stability and creep resistance can become limiting in certain extreme applications [6]. As a result, current research is moving towards new grades enriched with alloying elements such as nickel and chromium (which offer a significant improvement in terms of mechanical and electrochemical resistivity, thus favoring...) which improves electrical resistivity and enhances the formation of stable phases at high temperatures [7], paving the way for more demanding applications [8].

In this case, powder metallurgy (PM) is a particularly interesting process. It offers great control over microstructure, enhanced chemical homogeneity and near-net shape, while significantly reducing the amount of material lost [9]. Sintering, the heart of the MP process, consists

in consolidating metal powders by heating under pressure, without reaching melting temperature. Among the most advanced variants, Spark Plasma Sintering (SPS), also known as FAST (Field Assisted Sintering Technique), stands out for its rapid heating, short residence time at high temperature and ability to achieve high density in a short time [10, 11]. This technique can also be used to obtain ultra-fine microstructures and improve the mechanical performance of metastable titanium alloys [12]. It is particularly effective for refractory or segregation-sensitive materials, such as titanium alloys [13, 14].

In this context, the study is part of a strategy to develop a new Ti6Al2Ni2Cr-type titanium alloy for high-temperature applications. This system was developed by SPS from pure metal powders, with the aim of characterizing the influence of heat treatment on the material's mechanical and microstructural properties.

By combining advanced characterization techniques such as X-ray diffraction (XRD), scanning electron microscopy (SEM/EDS) and instrumented microhardness, we aim to assess the material's phase stability, structural homogeneity and mechanical aptitude. This research contributes to a deeper understanding of the synergistic effects of alloying elements and sintering conditions on final performance, with a view to optimization for the extreme conditions encountered in aerospace.

## 2 Materials and methods

### 2.1 Materials and sintering processes using SPS plasma sintering process

In this study, the alloy studied, with a nominal composition of Ti-6Al-2Cr-2Ni (in % by mass), was produced by SPS (Spark Plasma Sintering) from elemental powders with an average particle size of around 40  $\mu\text{m}$ . After grinding for 2 hours, a homogeneous mixture weighing 7 g of powder was introduced into a cylindrical graphite die (20 mm in diameter), with a SIGRAFLEX® graphite sheet (thickness 0.37 mm) placed between the punches and the mixture to ensure good thermal conductivity. Sintering was carried out using SPS equipment (FCT System GmbH) at the Physico-Chemical Research Center of the USTHB University (Algeria). The thermal cycle involved a temperature rise to 1000 °C at a rate of 100 °C/min, maintained for 10 minutes, under a constant uniaxial pressure of 30 MPa, in an argon atmosphere. Temperature was measured by optical pyrometer, 5 mm from the sample.

### 2.2 Microstructural analyses and mechanical properties

The sintered samples were first polished through a series of silicon carbide abrasive papers, followed by a final polish using a 0.25  $\mu\text{m}$  diamond paste. Microstructural observations were carried out using a JEOL® 7200F field-effect scanning electron microscope (FE-SEM), equipped with a Bruker-made X-Flash 6130 EDS detector and Espirit V1.9 software. FE-SEM imaging is taken in secondary electron mode (SED), and in backscattered mode (BED) to see phase homogeneity, as well as the distribution of alloying elements.

In order to identify the constitution of the crystalline phases of the samples processed by SPS and after the annealing treatment, X-ray diffraction (XRD) spectra were recorded using a Panalytical® Empyrean powder diffractometer, operating at 45 kV and 40 mA with Cu-K $\alpha$  radiation ( $\lambda = 1.54051 \text{ \AA}$ ) and  $2\theta$  diffraction angles ranging from 20° to 80° in Goni mode. All analyses were performed at a scan speed of 2 °/min. Crystalline phase identification is performed using PDF2 databases. To see the effect of annealing treatment on phase changes, quantitative phase analysis was carried out using the Rietveld method (references or two).

Microhardness measurements were carried out on polished surfaces using a Vickers indenter, with an applied load of 5 N for 15 seconds. Average values were calculated from a series of 10 measurements. The equipment used was a Zwick® ZHV10 with a CCD camera. Based on the indentation tests, the indentation modulus was calculated following the procedures described in section X4 of ASTM E2546-15 Standard [15]. A value of 0.3 was used for the Poisson's ratio of the tested materials.

## 3 Results and discussion

### 3.1 X-ray Diffraction (XRD)

DRX analysis carried out on samples of titanium-based alloys processed by Spark Plasma Sintering (SPS), with and without heat treatment, revealed the presence of the majority  $\alpha$ -Ti phase, accompanied by interstitial and intermetallic secondary phases.

For the sample after SPS sintering as shown in Fig. 1(a), X-ray diffraction revealed a predominance of the  $\alpha$ -Ti phase (87.1%) with a compact hexagonal structure (hcp), characterized by intense peaks located at  $2\theta \approx 38.4^\circ$ ,  $35.1^\circ$ , and  $40.25^\circ$ , typical of this structure, this high presence of Ti  $\alpha$  is expected in titanium alloys featuring  $\alpha$ -phase-stabilizing elements such as low-grade aluminum [16]. AlTi alloy, also hexagonal in structure, is present at 9.4%, indicating

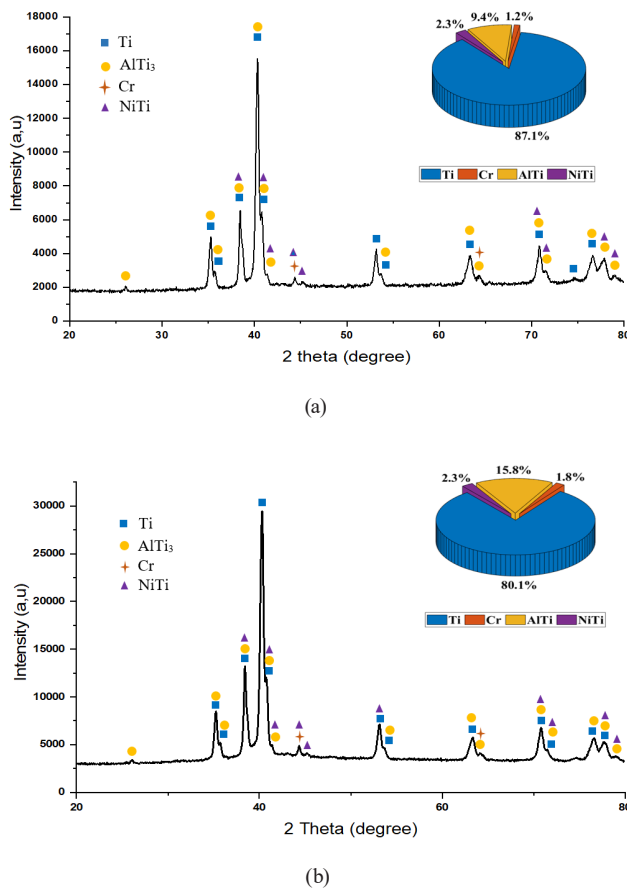


**Fig. 1** X-ray diffraction (XRD) spectra of Ti6Al2Cr2Ni alloy: (a) before heat treatment and (b) after annealing at 550 °C

a certain affinity between titanium and aluminum to form intermetallic compounds, particularly in areas where aluminum diffusion has been promoted by the localized heat of the SPS process. Minority phases such as NiTi (2.3%) and Cr (1.2%) are also identified. The presence of NiTi with a hexagonal structure may result from limited diffusion of nickel into the titanium matrix, with no visible martensitic transformation at this stage. Chromium appears in cubic form, probably as dispersed precipitates, as suggested by the low intensity of its peaks at 20.6° and 43.1° [17].

The heat-treated sample (annealed at 550 °C) shown in Fig. 1(b) demonstrates that this induced significant changes in phases and crystal structures. The percentage of the  $\alpha$ -Ti phase decreased to 80.1%, which could indicate a slight transformation or reaction of the  $\alpha$ -Ti phase with the additive elements in the matrix, favoring the growth of secondary phases. The intermetallic compound AlTi remains constant at 9.4%, retaining its hexagonal structure but appearing with a slight shift in the corresponding peaks (38.72°, 30.9°, 42.8°), which may reflect atomic reorganization or relaxation of internal stresses, due to the SPS

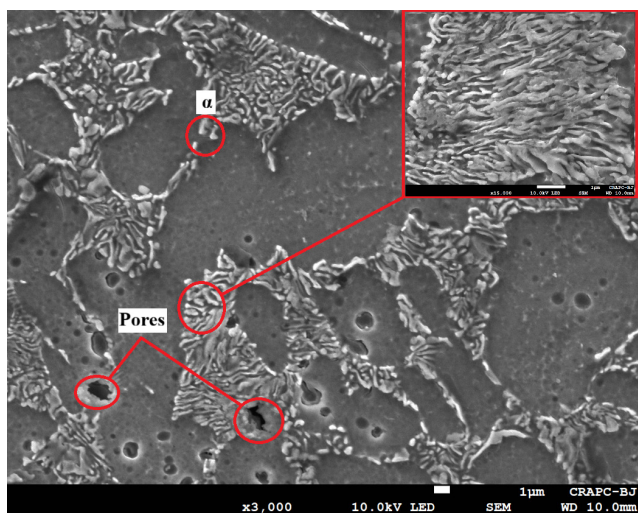
process. In addition, the NiTi phase underwent a significant transformation from a hexagonal to a monoclinic structure. This martensitic transformation is known to occur at low temperatures or following heat treatment, reflecting improved lattice organization and stronger interaction between Ni and Ti [18]. The peaks observed at 41.05°, 38.2° and 72.4° are typical of this monoclinic martensitic phase, often associated with a potential shape memory effect. Chromium also undergoes crystallographic transformation to a tetragonal structure (64.6° and 44.37°), suggesting possible precipitation of annealing-stabilized Cr-rich compounds, which could impact local hardness.

The dominant presence of the  $\alpha$ -Ti phase in both samples is in line with expectations for Ti-Al alloys with a low content of  $\beta$ -stabilizing elements. Heat treatment at 550 °C favors subtle crystal reorganizations and the formation of more thermodynamically stable intermetallic phases. This behavior has already been documented in several studies, where post-SPS treatments induce improved microstructural homogeneity and enhanced stability of the phases formed [19, 20]. The observation of the NiTi monoclinic phase after annealing is particularly interesting, as it could introduce functional effects (pseudo-elasticity, shape memory effect) into the alloy, in addition to its intrinsic mechanical properties. Furthermore, the transformation of Cr suggests local segregation or interaction with other elements, probably influenced by thermal diffusion kinetics [21].

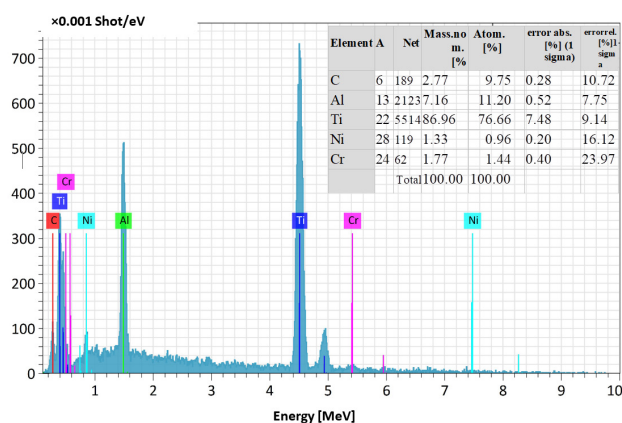
### 3.2 Scanning Electron Microscopy (SEM)

The SEM micrographs shown in Figs. 2 and 3 respectively illustrate the microstructure of the Ti6Al2Cr2Ni alloy before and after annealing heat treatment at 550 °C. Before heat treatment (Fig. 2), the microstructure is characterized by the significant presence of residual porosities, testifying to insufficient densification during the SPS process, visible segregation zones, reflecting an inhomogeneous distribution of alloying elements, probably due to limited diffusion at this stage of the process. The observation of well-developed  $\alpha$ -Ti phases, identifiable by their lamellar morphology, which is in agreement with X-ray diffraction results having identified predominantly the compact hexagonal  $\alpha$ -Ti phase (hcp) [22].

After heat treatment (Fig. 3), there was a noticeable reduction in porosity, attributed to thermal diffusion facilitated by annealing, resulting in improved intergranular cohesion and a more homogeneous microstructure, with partial disappearance of segregation zones. This homogenization can be linked to the increased diffusion of Cr and



(a)



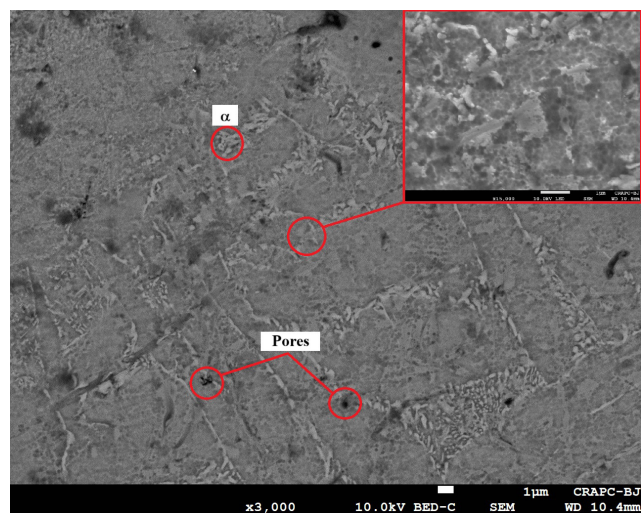
(b)

**Fig. 2** (a) SEM microstructural observations and (b) EDS mapping of the Ti-6Al-2Cr-2Ni alloy before heat treatment

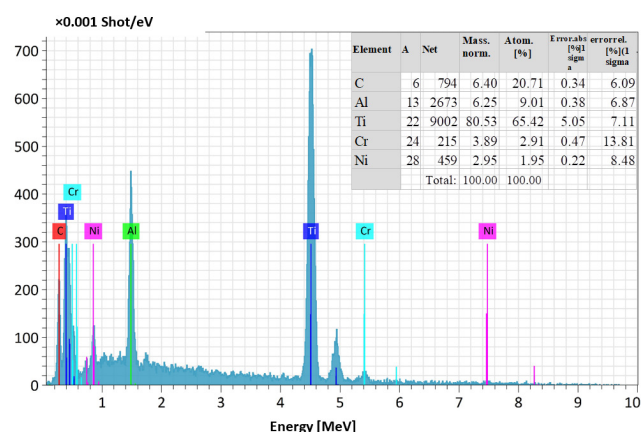
Ni elements at 550°C, which improves element redistribution [23], with the  $\alpha$  phase remaining dominant, confirming the stability of the hcp structure of aluminum- alloyed titanium, even after moderate heat treatment [24]. The overall improvement in microstructure after annealing potentially contributes to improved mechanical strength, including an increase in hardness observed in some similar cases [25].

EDS's spectrometry results confirm the electron microscopy observations. Before treatment (Fig. 2), the average chemical composition shows a majority titanium content by mass (86.96%), followed by aluminum (7.16%), carbon (2.77%), nickel (1.33%) and chromium (1.77%). The high titanium content is consistent with the nominal composition, but the low proportion of alloying elements and their heterogeneous distribution corroborate the presence of segregations observed in SEM.

After heat treatment (Fig. 3), EDS analyses show a decrease in titanium content (80.53%), with a slight



(a)



(b)

**Fig. 3** (a) SEM microstructural observations and (b) EDS mapping of the Ti-6Al-2Cr-2Ni alloy after heat treatment at 550 °C

increase in the proportions of Cr (3.89%) and Ni (2.95%). These trends indicate a better distribution of alloying elements, linked to the diffusion mechanisms activated during annealing. In addition, the decrease in carbon content suggests a partial relaxation of internal stresses and a local purification of the analyzed surface.

All these observations underline the effectiveness of heat treatment in improving the chemical homogeneity and microstructure of the Ti6Al2Cr2Ni alloy, which may reflect favorably on its mechanical properties.

### 3.3 Microhardness

Load-unload curves obtained by instrumented indentation on Ti6Al2Cr2Ni alloy, shown in Figs. 4(a) and 4(b), illustrate the evolution of the alloy's local mechanical behavior before and after thermal annealing at 550 °C. These curves provide valuable information on the material's microhardness and modulus of elasticity, reflecting the



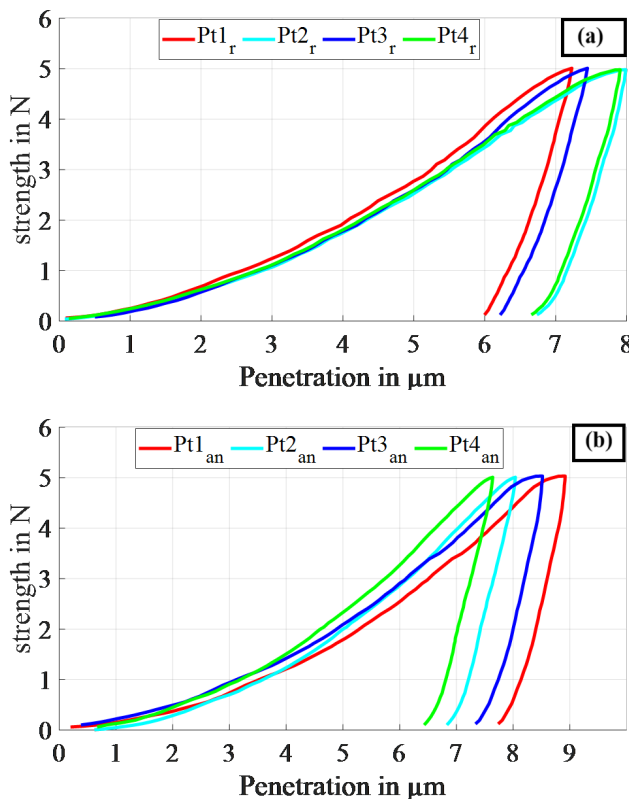


**Fig. 4** Load-discharge curves obtained by instrumented indentation on Ti6Al2Cr2Ni alloy, (a) without heat treatment, (b) after annealing treatment

microstructural changes induced by heat treatment. Before heat treatment; in the initial state, the loading curves reveal a progressive rise in applied force up to a maximum penetration depth of around 7.5 μm, with loads peaking at around 5.2 N. This behavior indicates an increased resistance to plastic deformation, characteristic of a hard material. The relatively steep slopes of the unloading curves suggest a high modulus of elasticity, reflecting a poorly relaxed crystal lattice and a high density of dislocations induced during SPS sintering. This phenomenon is common in high-temperature, high-pressure sintered materials, where the initial microstructure exhibits a degree of heterogeneity due to thermal gradients and rapid cooling rates [25]. After heat treatment; after annealing, the curves show an increase in maximum penetration depth, reaching up to 8.8 μm, for a similar load. This increase reflects a significant reduction in surface hardness, attributed to the relaxation of internal stresses and partial recrystallization that occurs during heat treatment. This evolution is corroborated by the studies of Gurrappa et al. [26], who observed a softening of titanium alloys after annealing, due to a reduction in dislocation density and a more thermodynamically stable atomic rearrangement. In addition, the slope of the unloading curves is lower after annealing,

indicating a drop in indentation modulus. This observation is in line with the work of Oliver and Pharr [27], who showed that slope variations in the unloading phase can be directly correlated to the material's elastic stiffness. In our case, the decrease in modulus reflects a transition to a more homogeneous, but less stressed microstructure, possibly with slight grain growth or a decrease in the density of active grain boundaries.

These results clearly show that heat treatment at 550 °C has significantly modified the alloy's local mechanical response. While hardness is slightly reduced, the microstructural stability obtained, coupled with good measurement reproducibility, indicates a potential for long-term performance optimization, particularly in applications where toughness and resistance to thermal fatigue are critical.

The results, shown in Fig. 5, reveal a significant increase in average microhardness after heat treatment compared to the untreated state. Before annealing, hardness values are lower and show some variability according to position. This response is generally attributed to an initial heterogeneous microstructure, characterized by a non-uniform distribution of phases formed during rapid sintering, as well as to the presence of porosities and residual stresses from the SPS process [28].

After annealing, hardness increases significantly in all positions measured. This behavior is explained by microstructural homogenization and improved diffusion of alloying elements, favoring the formation or growth of hard phases, such as NiTi and AlTi. In addition, the reduction in residual stresses and porosity, observed by scanning electron microscopy (SEM), contributes to improved resistance to local plastic deformation [29]. Annealing also

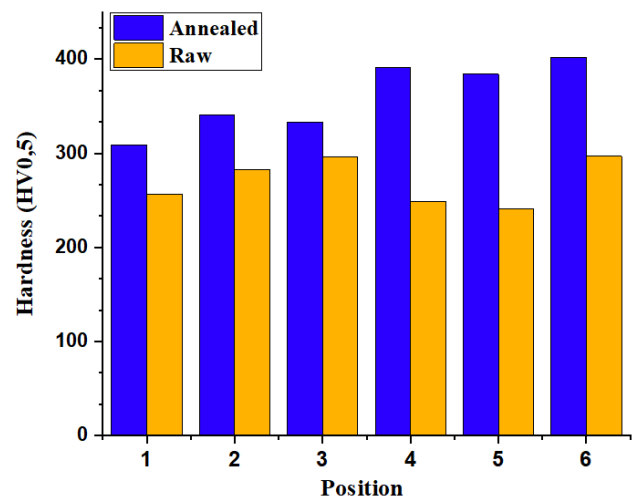


**Fig. 5** Histograms of microhardness at different positions before and after annealing

enables a microscopic rearrangement of atoms, increasing the density and thus the overall hardness of the alloy.

This behavior is in line with observations reported in the literature for titanium alloys modified with interstitial or substitution elements. In many cases, heat treatment can induce stabilization of the hard intermetallic phases, thus explaining the rise in hardness despite stress relaxation [30].

### 3.4 Young's modulus before and after annealing

Nanoindentation results showed a significant increase in Young's modulus after heat treatment at 550 °C, from 185 GPa to 190 GPa as indicated in Fig. 6. This reflects an improvement in the elastic stiffness of the Ti-6Al-2Cr-2Ni alloy, which can be explained by a synergy between microstructural evolution and annealing-induced chemical redistribution. DRX analysis revealed an intensification of peaks associated with the  $\alpha$ -Ti phase and a reduction in contributions from secondary phases such as; AlTi and NiTi after annealing, suggesting improved phase stability. This transformation favors a more homogeneous elastic behavior, consistent with the observations of [31].

SEM images confirm this interpretation, showing increased matrix densification after annealing and a significant reduction in intergranular porosity. These observations indicate an improvement in structural cohesion and a reduction in local heterogeneities, factors directly correlated with the rise in Young's modulus. In addition, EDS mapping before and after heat treatment revealed a more uniform chemical distribution of Cr and Ni in the matrix. This is crucial, as chemical homogeneity reduces local stress concentrations and promotes the overall mechanical stability of the material [32].

From a microhardness point of view, the tests showed a

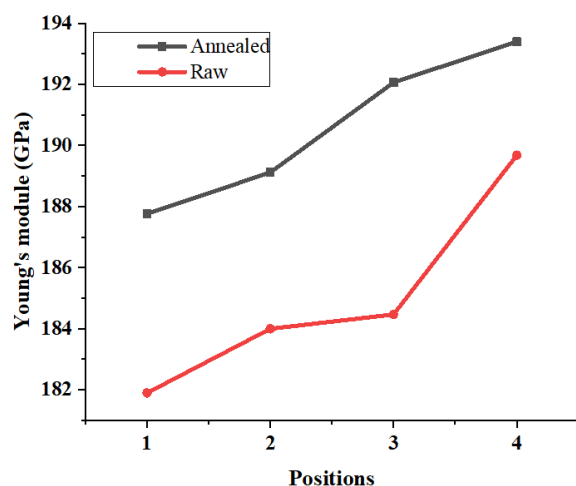


Fig. 6 Young's modulus before and after annealing

slight increase in hardness after annealing (from ~355 HV to ~370 HV), consistent with the more pronounced presence of  $\text{Ti}_2\text{Ni}$  type precipitates identified by DRX. These precipitates strengthen the  $\alpha$ -Ti matrix through dispersion hardening, indirectly contributing to the increase in elastic modulus. As reported by Ghosh et al. [22], such controlled precipitation stabilizes mechanical properties while maintaining good ductility.

In short, the increase in Young's modulus results from a coherent set of modifications: microstructural densification, chemical homogenization, phase transformation and fine precipitation. These mechanisms have already been described in the literature as beneficial for titanium alloys obtained by SPS [33]. Thus, the heat-treated Ti-6Al-2Cr-2Ni alloy is positioned as a promising material for aerospace applications requiring high mechanical stability under thermal load.

## 4 Conclusion

This study evaluated the influence of annealing at 550 °C on the microstructural and mechanical properties of a Ti-6Al-2Cr-2Ni alloy produced by Spark Plasma Sintering (SPS).

- SEM observations revealed a more homogeneous microstructure after heat treatment, accompanied by a significant reduction in porosity.
- EDS analysis confirmed a better distribution of alloying elements (Al, Cr, Ni) in the matrix, reflecting a chemical homogenization favorable to the stability of mechanical properties.
- X-ray diffraction (XRD) results highlighted a predominance of the  $\alpha$ -Ti phase, as well as the presence of secondary phases such as  $\text{Ti}_2\text{Ni}$ , AlTi and NiTi.
- Microhardness tests showed a slight increase in hardness after annealing, attributed to the precipitation of reinforcing phases and a reduction in residual stresses.
- Finally, the nanoindentation tests revealed an improvement in Young's modulus, rising from 185 GPa to 190 GPa, confirming the strengthening of the material's rigidity in line with the microstructural evolution.

In conclusion, the heat treatment applied to SPS-sintered Ti-6Al-2Cr-2Ni optimizes compactness, promotes phase stability, and improves overall mechanical properties, particularly elastic stiffness. These results position this alloy as a relevant material for aerospace applications, where mechanical strength and reliability at high temperatures are essential.

## References

- [1] Wang, Q., Zhang, X., Jia, X., He, Y., Zhou, J., Sun, Y., Cheng, X. "Microstructure, Mechanical Properties at Room Temperature and High Temperature of Near- $\alpha$  Titanium Alloys Fabricated by Spark Plasma Sintering", *Nanomaterials*, 15(4), 293, 2025.  
<https://doi.org/10.3390/nano15040293>
- [2] Digole S., Karki, S., Mugale, M., Choudhari, A., Gupta, R. K., Borkar, T. "Spark Plasma Sintering of Pure Titanium: Microstructure and Mechanical Characteristics", *Materials*, 17(14), 3469, 2024.  
<https://doi.org/10.3390/ma17143469>
- [3] Zyguła, K., Lypchanskyi, O., Łukaszek-Solek, A., Korpała, G., Stanik, R., Kubiś, M., Przybyszewski, B., Wojtaszek, M., Gude, M., Prah, U. "A Comprehensive Study on Hot Deformation Behavior of the Metastable  $\beta$  Titanium Alloy Prepared by Blended Elemental Powder Metallurgy Approach", *Metallurgical and Materials Transactions A*, 55(3), pp. 933–954, 2024.  
<https://doi.org/10.1007/s11661-024-07297-9>
- [4] Banerjee, D., Williams, J. C. "Perspectives on Titanium Science and Technology", *Acta Materialia*, 61(3), pp. 844–879, 2013.  
<https://doi.org/10.1016/j.actamat.2012.10.043>
- [5] Fang, Z. Z., Paramore, J. D., Sun, P., Ravi Chandran, K. S., Zhang, Y., Xia, Y., Cao, F., Koopman, M., Free, M. "Powder Metallurgy of Titanium – Past, Present, and Future", *International Materials Reviews*, 63(7), pp. 407–459, 2018.  
<https://doi.org/10.1080/09506608.2017.1366003>
- [6] Groza, J. R., Zavaliangos, A. "Sintering Activation by External Electrical Field", *Materials Science and Engineering A*, 287(2), pp. 171–177, 2000.  
[https://doi.org/10.1016/S0921-5093\(00\)00771-1](https://doi.org/10.1016/S0921-5093(00)00771-1)
- [7] Wang, H., Chen, W., Chu, C., Fu, Z., Jiang, Z., Yang, X., Lavernia, E. J. "Microstructural Evolution and Mechanical Behavior of Novel Ti1.6ZrNbAlx Lightweight Refractory High-Entropy Alloys Containing BCC/B2 Phases", *Materials Science and Engineering A*, 885, 145661, 2023.  
<https://doi.org/10.1016/j.msea.2023.14566>
- [8] Gomez-Gallegos, A., Mandal, P., Gonzalez, D., Zuelli, N., Blackwell, P. "Studies on Titanium Alloys for Aerospace Application", *Defect and Diffusion Forum*, 385, pp. 419–423, 2018.  
<https://doi.org/10.4028/www.scientific.net/DDF.385.419>
- [9] Peters, M., Kumpfert, J., Ward, C. H., Leyens, C. "Titanium Alloys for Aerospace Applications", *Advanced Engineering Materials*, 5(6), pp. 419–427, 2003.  
<https://doi.org/10.1002/adem.200310095>
- [10] Wang, Y., Zhao, H., Ma, H., Zhang, Y. "The effect of thickness on fracture characteristics of TC4 titanium alloy sheets", *Archives of Civil and Mechanical Engineering*, 22(4), 151, 2022.  
<https://doi.org/10.1007/s43452-022-00473-x>
- [11] Ren, Y., Cao, Y., Liu, Y., Jie, Z., Jian, Z., ..., Huang, W. "Fracture toughness of titanium alloys fabricated by high-power laser-directed energy deposition: Fractal analysis and prediction model", *Journal of Materials Science & Technology*, 228, pp. 54–74, 2025.  
<https://doi.org/10.1016/j.jmst.2024.12.027>
- [12] Motyka, M. "Martensite Formation and Decomposition during Traditional and AM Processing of Two-Phase Titanium Alloys – An Overview", *Metals*, 11(3), 481, 2021.  
<https://doi.org/10.3390/met11030481>
- [13] Lee, S., Park, C., Hong, J., Yeom, J.-T. "The Role of Nano-domains in {1–011} Twinned Martensite in Metastable Titanium Alloys", *Scientific Reports*, 8(1), 11914, 2018.  
<https://doi.org/10.1038/s41598-018-30059-8>
- [14] Ma, G., Yu, C., Tang, B., Li, Y., Niu, F., Wu, D., Bi, G., Liu, S. "High-mass-proportion TiCp/Ti6Al4V titanium matrix composites prepared by directed energy deposition", *Additive Manufacturing*, 35, 101323, 2020.  
<http://doi.org/10.1016/j.addma.2020.101323>
- [15] Lu S., Medvedev A., Qiu D., Song T., Brandt M., Qian M. "The Intricacies of  $\alpha$ - $\beta$  Microstructures in Titanium Alloys: Insights into  $\alpha$ -Phase Variant Spatial Distribution and Orientation", *Scripta Materialia*, 263, 116690, 2025.  
<https://doi.org/10.1016/j.scriptamat.2025.116690>
- [16] Huang, S., Zhao, Q., Yang, Z., Lin, C., Zhao, Y., Yu, J. "Strengthening effects of Al element on strength and impact toughness in titanium alloy", *Journal of Materials Research and Technology*, 26, pp. 504–516, 2023.  
<https://doi.org/10.1016/j.jmrt.2023.07.206>
- [17] Otsuka, K., Ren, X. "Physical Metallurgy of Ti–Ni-Based Shape Memory Alloys", *Progress in Materials Science*, 50(5), pp. 511–678, 2005.  
<https://doi.org/10.1016/j.pmatsci.2004.10.001>
- [18] Li, Y., Liao, Q., Song, Y., Yang, Y. "Effect of Heat Treatment on the Microstructure and Mechanical Properties of Investment Casting Ti-1300 Alloy", *Metallurgical and Materials Transactions A*, 55(10), pp. 4190–4199, 2024.  
<https://doi.org/10.1007/s11661-024-07544-z>
- [19] Xue, G.-L., Xing, H.-X., Ye, C., Liu, J. "Effect of Ti on Microstructure, Mechanical Properties and Corrosion Resistance of Zr-Ta-Ti Alloys Processed by Spark Plasma Sintering", *Journal of Central South University*, 27(8), pp. 2185–2197, 2020.  
<https://doi.org/10.1007/s11771-020-4440-9>
- [20] Klein, M., Staufer, E., Edtmaier, C., Horky, J., Schmitz-Niederau, M., Zhang, D., Qiu, D., Easton, M., Klein, T. "Effects of Heat Treatment and Processing Conditions on the Microstructure and Mechanical Properties of a Novel Ti–6.3Cu–2.2Fe–2.1Al Alloy", *Advanced Engineering Materials*, 26(16), 2400534, 2024.  
<https://doi.org/10.1002/adem.202400534>
- [21] Sun, J., Qi, M., Zhang, J., Li, X., Wang, H., Ma, Y., Xu, D., Lei, J., Yang, R. "Formation Mechanism of  $\alpha$  Lamellae During  $\beta \rightarrow \alpha$  Transformation in Polycrystalline Dual-Phase Ti Alloys", *Journal of Materials Science & Technology*, 71, pp. 98–108, 2021.  
<https://doi.org/10.1016/j.jmst.2020.02.093>
- [22] Ghosh, M., Bhanumurthy, K., Kale, G. B., Krishnan, J., Chatterjee, S. "Diffusion Bonding of Titanium to 304 Stainless Steel", *Journal of Nuclear Materials*, 322(2), pp. 235–241, 2003.  
<https://doi.org/10.1016/j.jnucmat.2003.07.004>

- [23] Despax, L., Vidal, V., Delagnes, D., Dehmas, M., Matsumoto, H., Velay, V. "Mechanical Behaviour and Microstructural Evolution in Fine Grain Ti-6Al-4V Alloy under Superplastic Conditions", MATEC Web of Conferences, 321, 11011, 2020.  
<https://doi.org/10.1051/mateconf/202032111011>
- [24] Fu, Z., MacDonald, B. E., Monson, T. C., Zheng, B., Chen, W., Lavernia, E. J. "Influence of Heat Treatment on Microstructure, Mechanical Behavior and Soft Magnetic Properties in an FCC-Based  $\text{Fe}_{29}\text{Co}_{28}\text{Ni}_{29}\text{Cu}_7\text{Ti}_7$  High-Entropy Alloy", Journal of Materials Research, 33(15), pp. 2214–2222, 2018.  
<https://doi.org/10.1557/jmr.2018.161>
- [25] Yadav, P., Saxena, K. K. "Effect of Heat Treatment on Microstructure and Mechanical Properties of Ti Alloys: An Overview", Materials Today Proceedings, 26, pp. 2546–2557, 2020.  
<https://doi.org/10.1016/j.matpr.2020.02.541>
- [26] Yu, H., Hu, Q., Huang, Y., Zeng, Y., Jia, J., Hu, Q., Hing, R., Zhang, Y. "Enhanced Mechanical Properties Via the Incorporation of Ti in Cu Alloys", Archives of Metallurgy and Materials, 69(4), pp. 1345–1352, 2025.  
<https://doi.org/10.24425/amm.2024.151398>
- [27] Ezatpour, H. R., Torabi-Parizi, M. "Effect of Ti Content on Achieving Development of Mechanical Properties and Wear Resistance of CoCrFeNiMoTi<sub>x</sub> High Entropy Alloy", Journal of Materials Research and Technology, 29, pp. 5447–5463, 2024.  
<https://doi.org/10.1016/j.jmrt.2024.03.018>
- [28] Pan, K., Liu, X., Wang, B., Gao, S., Wu, S., Li, N. "The Rapid Densification Behavior of Powder Metallurgy Ti Alloys by Induction Heating Sintering", Journal of Materials Science & Technology, 181, pp. 152–164, 2024.  
<https://doi.org/10.1016/j.jmst.2023.10.009>
- [29] Chaudhari, R., Bauri, R. "Microstructure and Mechanical Properties of Titanium Processed by Spark Plasma Sintering (SPS)", Metallography, Microstructure, and Analysis, 3(1), pp. 30–35, 2014.  
<https://doi.org/10.1007/s13632-013-0112-6>
- [30] Mercier, S., Molinari, A. "Homogenization of Elastic–Viscoplastic Heterogeneous Materials: Self-Consistent and Mori–Tanaka Schemes", International Journal of Plasticity, 25(6), pp. 1024–1048, 2009.  
<https://doi.org/10.1016/j.ijplas.2008.08.006>
- [31] Li, J., Zhang, M., Li, B., Monteiro, S. N., Ikhmayies, S., Kalay, Y. E., Hwang, J.-Y., Escobedo-Diaz, J. P., Carpenter, J. S., Brown, A. D. (eds.) "Characterization of Minerals, Metals, and Materials 2020", Springer Cham, 2020. ISBN 978-3-030-36628-5  
<https://doi.org/10.1007/978-3-030-36628-5>
- [32] Qiu, D., Shi, R. "Effect of Modulus Heterogeneity on the Equilibrium Shape and Stress Field of  $\alpha$  Precipitate in Ti-6Al-4V", Computer Modeling in Engineering & Sciences, 140(1), pp. 1017–1028, 2024.  
<https://doi.org/10.32604/cmescs.2024.048797>
- [33] Boulnat, X. "Consolidation rapide à haute température d'aciers renforcés par dispersion d'oxydes (ODS) : Procédé, microstructure, précipitation, propriétés mécaniques" (FAST high-temperature consolidation of Oxide-Dispersion Strengthened (ODS) steels: Process, microstructure, precipitation, properties), PhD thesis, Institut National de Sciences Appliquées Lyon, 2014. (In French)